INL/CON-08-14932
PREPRINT

# Use of Multiple Reheat Helium Brayton Cycles to Eliminate the Intermediate Heat Transfer Loop for Advanced Loop Type SFRs

## ICAPP '09

Haihua Zhao
Hongbin Zhang
Samuel E. Bays

May 2009



Proceedings of ICAPP '09
Tokyo, Japan, May 10-14, 2009
Paper 9026

# Use of Multiple Reheat Helium Brayton Cycles to Eliminate the Intermediate Heat Transfer Loop for Advanced Loop Type SFRs

Haihua Zhao*, Hongbin Zhang, and Samuel E. Bays
Idaho National Laboratory
*Idaho National Laboratory, PO BOX 1625, Idaho Falls, ID 83415-3870, USA
Tel: +1 (208)526-2679, Fax: +1 (208) 526-0528, Email: Haihua.Zhao@inl.gov*

**Abstract** - *The sodium intermediate heat transfer loop is used in existing sodium cooled fast reactor (SFR) plant design as a necessary safety measure to separate the radioactive primary loop sodium from the water of the steam Rankine power cycle. However, the intermediate heat transfer loop significantly increases the SFR plant cost and decreases the plant reliability due to the relatively high possibility of sodium leakage. A previous study shows that helium Brayton cycles with multiple reheat and intercooling for SFRs with reactor outlet temperature in the range of 510°C to 650°C can achieve thermal efficiencies comparable to or higher than steam cycles or recently proposed supercritical $CO_2$ cycles. Use of inert helium as the power conversion working fluid provides major advantages over steam or $CO_2$ by removing the requirement for safety systems to prevent and mitigate the sodium-water or sodium-$CO_2$ reactions. A helium Brayton cycle power conversion system therefore makes the elimination of the intermediate heat transfer loop possible. This paper presents a pre-conceptual design of multiple reheat helium Brayton cycle for an advanced loop type SFR. This design widely refers the new horizontal shaft distributed PBMR helium power conversion design features. For a loop type SFR with reactor outlet temperature 550°C, the design achieves 42.4% thermal efficiency with favorable power density comparing with high temperature gas cooled reactors.*

## I. INTRODUCTION

Achieving economic competitiveness as compared to LWRs and other Generation IV (Gen-IV) reactors is one of the major requirements for large-scale investment in commercial Sodium Cooled Fast Reactor (SFR) power plants. SFR economics can be improved both through reducing capital cost and increasing plant availability. There are many ways to reduce capital cost, for example: simplifying design, using innovative passive design, using advanced components, using advanced material and fuel, or increasing power to take advantage of economics of scale, etc. Past and current SFR programs often utilize multiple methods to reduce capital cost. For example, European Fast Reactor (EFR)[1] program simplified the primary system and pushed the power to 3600 MWt based on past European experiences, especially Superphenix[2]. JSFR[3,4] also takes advantage of economics of scale, use fewer number of loops and shorter pipes. All these efforts reduce the SFR capital cost. Further cost reduction efforts are still on going.

SFR availability also needs to be increased to the level of LWRs. Currently, the US LWR fleet has consistently achieved a capacity factor above 90%. Although successful operating experience with past and existing test and prototype SFRs has demonstrated generally good safety and reliability, incidents and failures did occur in these prototype reactors and plants.[2,5] The Russian BN-600 achieved 75% capacity factor, which is the best record for SFRs. Even it had recorded a number of sodium leakage incidents, some involved sodium-water reactions. These incidents limited the SFR's capability to achieve high availability.

One option to reduce capital cost and simultaneously to increase SFR availability is to eliminate the intermediate sodium heat transfer loop. The sodium intermediate heat transfer loop is used in existing SFR plant designs as a necessary safety measure to separate the radioactive primary loop sodium from the water of the steam Rankine power cycle. However, the intermediate heat transfer loop significantly increases the SFR plant cost and decreases the plant reliability due to the relatively high possibility of sodium leakage. For example, reference 5 shows that quite a few sodium leakage accidents in the intermediate sodium loop and sodium water reaction accidents happened in test and demonstration SFRs. These accidents often involved sodium fire and violent water sodium reactions and some resulted in very long time shutdown.[6] Suppression of the intermediate heat transfer system has been a focus of further cost reduction in the fast reactor community.

Eliminating the intermediate sodium loop needs to consider the selection of power conversion systems. If the traditional steam Rankine cycle is used, the steam generator must be extremely reliable and a very effective sodium-water detection and mitigation system is necessary. Several designs[7] proposed to use double walled tube steam generators so that the intermediate sodium loop can be eliminated. Such ideas may carry very large risks. Although limited experiences of using double walled tube steam generators in small test SFRs, such as EBR-II[8], show no leakage, for large commercial plants, the heat transfer area is very large and therefore the failure possibility increases proportionally. Even a quick sodium release and isolation system can be designed, the reactor primary system still needs circulation of sodium to cool the fuel. Simply dumping sodium into a big tank like the current design is not a viable solution any more.

Due to the safety concerns over steam cycles, alternative power cycles are being explored in new SFR designs. SCO2 recompression Brayton cycles[9] are recently proposed as power conversion systems by several advanced sodium fast reactor designs, such as US ABTR design[10]. A similar compatibility problem exists between sodium and $CO_2$ as with water.[11] The energetic reaction of $CO_2$ with sodium will generate even higher temperatures than sodium-water reactions and the major products include CO and the molten salt of $Na_2CO_3$. CO is a toxic gas, which may threaten the safety of plant workers; $Na_2CO_3$ could block pipes and contaminate the IHX. If a large amount of sodium reacts with $CO_2$, the released energy may threaten the integrity of the primary loop. Due to the severe nature of the Na-$CO_2$ reaction, it can be anticipated that expensive and complex safety systems will be required, which may significantly increase the capital cost. Without intermediate sodium loops, the safety risk will become even higher.

Inert gas power conversion systems have been sought to replace incompatible power conversion fluids like water and $CO_2$. French researchers studied several inert gas Brayton cycles, like helium, argon, nitrogen, or their mixtures.[12] Those simple Brayton cycles have much lower thermal efficiencies than SCO2 and steam cycles. Therefore, there are economic penalties related to lower thermal efficiency. The solution to the lower efficiency problem is through multiple reheat.[13, 14, 15] Recent studies[16, 17] show that multiple reheat helium Brayton cycles for SFRs can achieve similar or better thermal efficiency than steam or SCO2 cycles for the reactor outlet temperature in the range of 510°C to 650°C. Those designs keep the intermediate sodium heat transfer loop. An integral vertical shaft power conversion unit (PCU) configuration is adopted, similar as GT-MHR design[18]. Distributed horizontal shaft designs can be derived from PBMR design[19]. Fig. 1 compares four different power conversion systems. The top two, the PCUs for GT-MHR and PBMR, are middle power level Brayton cycles without reheat. The bottom two, an integral vertical shaft configuration and another horizontal distributed shaft configuration for SFRs, are large power level Brayton cycles with multiple-reheat. In Fig. 1, the systems on the left are vertical shaft and integrated systems; and the systems on the right are horizontal shaft and distributed systems. The success of HTGR (High Temperature Gas cooled Reactor) programs, like the GT-MHR, PBMR, and Japan's GTHTR300[20], will solve most technology challenges and demonstrate key enabling technologies for helium Brayton cycles, such as high temperature compact heat exchangers, high efficiency helium turbomachinery, advanced bearing and seals, and large high temperature ducting systems, etc. The optimal development path for larger multi-reheat systems can then be established based on those experiences and lessens learned from non-reheat version smaller Brayton cycle power conversion systems.

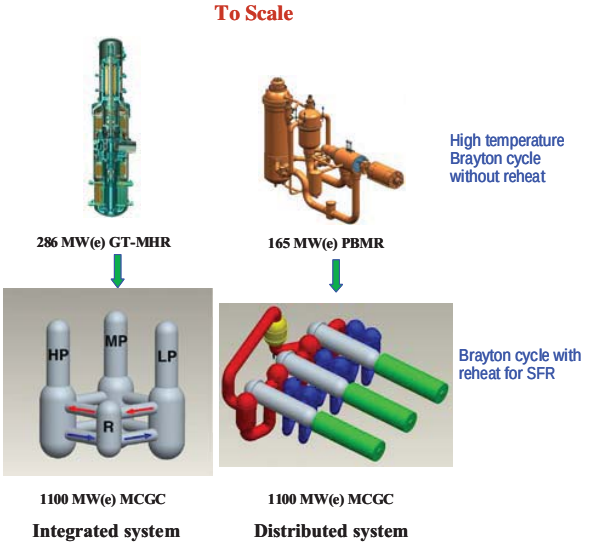


Fig. 1. Scaled comparison of four Brayton power conversion systems.

Use of inert helium as the power conversion working fluid provides major advantages over steam or $CO_2$ by removing the requirement for safety systems to prevent and mitigate the sodium-water or sodium-$CO_2$ reactions. A helium Brayton cycle power conversion system also makes the elimination of the intermediate heat transfer loop possible. Without the intermediate loop, intermediate heat exchangers (IHX) are also heaters for the multiple reheat helium cycle. Even for compact heat exchangers, the sodium-to-helium heaters still have large volume so that a pool type SFR configuration tends to have a very large sodium tank. This is not an issue for a loop type SFR design where the reactor core and IHXs (heaters) are in separate vessels.

Fig.2 shows the schematic of an advanced SFR plant for a loop type SFR with a multiple reheat helium Brayton cycle. The SFR primary design is similar as JSFR but with an optimized reactor inlet temperature to best couple with

the Brayton cycle. The helium Brayton cycle shown here only demonstrates the major components and flow path, not representing the best PCU arrangement, which will be described in later section. Note that heaters (primary sodium to helium IHX) are near the reactor vessel so that the primary system size can be minimized. To do so will result in long connection ducts between heaters and turbines as shown in the figure.

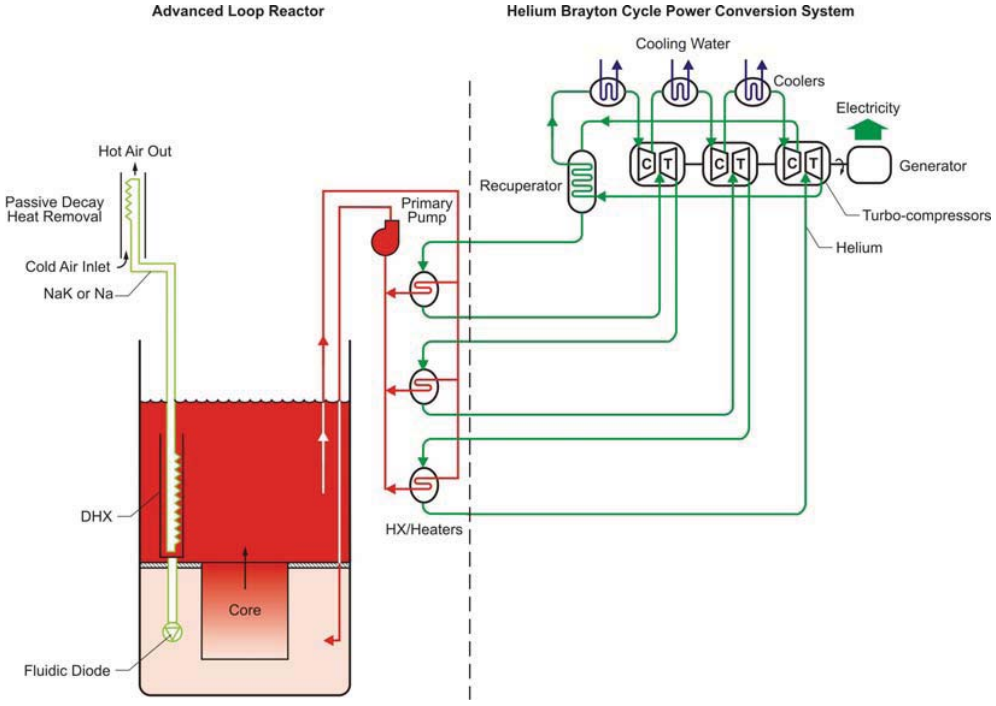


Fig. 2. An advanced loop type SFR with a multiple reheat helium Brayton cycle.

The following section will introduce multiple reheat helium cycle, including basic principle, thermodynamic design and system design method. Section III will present a pre-conceptual design of multiple reheat helium Brayton cycle for an advanced loop type SFR. Section IV will discuss some potential issues and further research needs. Section V summarizes the paper.

## II. MULTIPLE REHEAT HELIUM CYCLES THEORY AND DESIGN METHODS

### *II.A. Introduction and Theory*

It has been known in theory that reheat can increase the thermal efficiency for a closed gas Brayton cycle. However, only after the matureness of gas turbine technology and development of helium Brayton cycles for HTGRs, multiple reheat closed gas Brayton cycle began to be fully studied based on those advances. Peterson developed the original thermodynamical analysis.[13] By utilizing reheat, these multiple reheat molten coolant gas cycles (MCGC) have the potential for substantially higher thermal efficiency than current gas cooled reactors, if used with comparable turbine inlet temperatures.

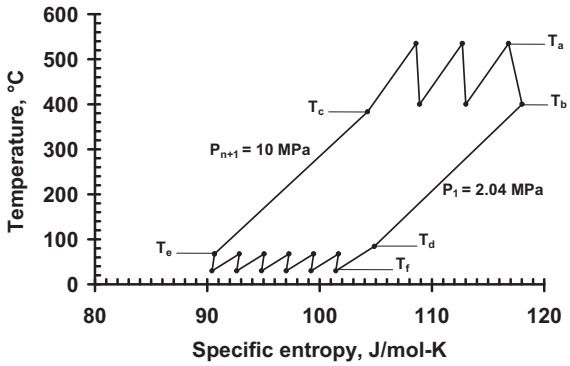


Fig. 3. Temperature-entropy diagram for the MCGC reference case; $T_a$ is the turbine inlet temperature, $T_b$ the turbine outlet temperature, $T_c$ the recuperator high-pressure side outlet temperature, $T_d$ the recuperator low-pressure side outlet temperature, $T_e$ the compressor outlet temperature, and $T_f$ the compressor inlet temperature.

Fig. 3 shows a temperature-entropy (T-s) diagram for an optimized MCGC reference design for a loop type SFR with 3 expansion stages and 6 compression stages, which shows the basic idea of a MCGC cycle. With multiple reheat stages, the average heat absorbing temperature is close to the highest heat source temperature; and with

multiple cooling stages, the average heat rejection temperature is close to the heat sink temperature. The heat transfer in the recuperator is internal, and does not affect the average heat input and heat rejection temperatures. The thermal efficiency for this optimized reference design shown in the figure is 42.4% at a turbine inlet temperature of 535ºC ($T_a$ in Figure 3). The thermal efficiency considers turbomachinary losses, pressure losses, and recuperator effectiveness but does not include other losses such as heat loss, generator and gear box (if used) losses, pumping power for cooling systems, and other plant house load. Note that the heating temperature range (from $T_c$ to $T_a$ and from $T_b$ to $T_a$ in Fig. 3) matches the SFR reactor inlet and outlet temperature range very well.

As shown in Figure 3, for an optimal cycle the multiple-reheat turbines are sized to provide equal pressure expansion ratios. The gas entering each turbine is heated to the same inlet temperature, using the heating source coolant in a counter-flow heat exchanger. Likewise the compressors are sized to provide equal compression ratios. The gas entering each compressor is cooled to the same temperature, using water in a counter-flow heat exchanger. The original study by Peterson[13] provided equations for analyzing the thermal efficiency of the MCGC, which are summarized below.

$$\frac{W_t}{M} = \left(T_a - T_b\right) = \eta_t \left(T_a - T_{bs}\right) \tag{1}$$

$$\frac{W_c}{M} = \left(T_e - T_f\right) = \frac{\left(T_{es} - T_f\right)}{\eta_c} \tag{2}$$

where $W$ is the power, $M$ the mass flow rate times specific heat, $T$ absolute temperature, $\eta_t$ the turbine efficiency, and $\eta_c$ the compressor efficiency. The definition of $T_a$, $T_b$, $T_c$, $T_d$, $T_e$ and $T_f$ are shown in Figure 3. The total pressure ratio for the cycle is then

$$\frac{P_{n+1}}{P_1} = \pi_c \left(\frac{T_{es}}{T_f}\right)^{\frac{n\gamma}{\gamma-1}} = \left(\frac{T_a}{T_{bs}}\right)^{\frac{m\gamma}{\gamma-1}} \tag{3}$$

where $P$ is pressure, $\gamma$ the gas constant, assumed to be constant, $n$ the number of compression stages, $m$ the number of expansion stages, and

$$\pi_c = 1 - \frac{\Delta P}{P_{n+1}} \tag{4}$$

corrects for system pressure losses $\Delta P$. Then for specified turbine inlet and outlet temperatures, and compressor inlet temperature, the compressor outlet temperature $T_e$ can be determined from Eqs. (1-3) as,

$$\frac{P_{n+1}}{P_1} = \pi_c \left(1 + \eta_c \left(\frac{T_e}{T_f} - 1\right)\right)^{\frac{n\gamma}{\gamma-1}} = \left(1 - \frac{1}{\eta_t}\left(1 - \frac{T_b}{T_a}\right)\right)^{-\frac{m\gamma}{\gamma-1}} \tag{5a}$$

$$T_e = T_f \left\{1 + \frac{1}{\eta_c}\left[\pi_c^{-\frac{\gamma-1}{n\gamma}}\left(1 - \frac{1}{\eta_t}\left(1 - \frac{T_b}{T_a}\right)\right)^{-\frac{m}{n}} - 1\right]\right\} \tag{5b}$$

The thermal efficiency $\eta_{MR}$ can be determined from the heat added $Q_H$ and the net work produced $W_n$,

$$\frac{Q_H}{M} = m\left(T_a - T_b\right) + \Delta T_r \tag{6}$$

$$\frac{W_n}{M} = \left[m\left(T_a - T_b\right) - n\left(T_e - T_f\right)\right] \tag{7}$$

$$\eta_{MR} = \frac{W_n}{Q_H} = \frac{1 - \frac{n}{m}\left(\frac{T_e - T_f}{T_a - T_b}\right)}{1 + \frac{\Delta T_r}{m\left(T_a - T_b\right)}} \tag{8}$$

$$\eta_{MR} = \frac{W_n}{Q_H} = \frac{1 - \frac{T_f}{\left(T_a - T_b\right)\eta_c}\frac{n}{m}\left[\pi_c^{-\frac{\gamma-1}{n\gamma}}\left(1 - \frac{1}{\eta_t}\left(\frac{T_a - T_b}{T_a}\right)\right)^{-m/n} - 1\right]}{1 + \frac{\Delta T_r}{m\left(T_a - T_b\right)}} \tag{9}$$

where the average temperature drop across the recuperator $\Delta T_r$ is related to the recuperator effectiveness $\eta_r$ as

$$\Delta T_r = \left(T_b - T_c\right) = \left(T_d - T_e\right) = \left(1 - \eta_r\right)\left(T_b - T_e\right) \tag{10}$$

As a first order of approximation, one can use the following estimation for the total fractional pressure loss (total pressure loss over system pressure) coefficient:

$$\pi_c = 1 - \left(c_r + c_T \cdot m + c_C \cdot n\right), \tag{11}$$

For the first iteration in solving for thermal efficiency, $c_r$=*0.01* is used for the fractional pressure loss for recuperator, $c_T$=*0.014* fractional pressure loss for one stage of heating and expansion (heater, turbine, and related ducting loss), and $c_C$=*0.007* fractional pressure loss for one stage of cooling and compression (cooler, compressor, and related ducting loss). These parameter values are only used as the initial estimation of system fractional pressure loss. After detailed designs for major components such as turbomachinary, heaters, coolers, recuperator, and ducting system are finished, the fractional pressure loss value is updated according to the sum of each component's pressure loss.

Using these equations, a parametric search was used to identify promising design parameters under SFR-relevant design constrains.

### *II.B. Summary of Component Designs*

A set of design and analysis Mathcad codes were developed to size the major components and analyze the system performance. These include:

- cycle thermal dynamical analysis code – which calculates the thermal efficiency, finds optimal values, and performs sensitivity analysis;
- compact heat exchanger design code – given thermal input data, calculates the total heat transfer area, pressure losses, and selects the heat exchanger module sizes;
- turbomachinery sizing code – estimates the sizes and pressure losses of all the turbines and compressors;
- duct system sizing code – calculates the connection duct size and pressure losses;
- material input code – estimates total helium inventory, total solid material input, and calculate the power density and specific steel input;
- properties database code – contain extensive collections of the solid and fluid physical and transport properties, including helium, sodium, high temperature alloys used in PCS design.

The cycle thermal dynamics analysis code is developed based on MCGC analysis equations list from 1 to 11. Input data are based on GT-MHR or PBMR PCS system parameters and component design results.

The compact heat exchanger design code can size either Printed Circuit Heat Exchanger (PCHE) or Plate Fin Heat Exchangers (PFHE). LMTD design procedures[21] are used to size heat exchangers and calculate pressure losses. The recuperator (helium to helium) is assumed to be an offset fin plate heat exchanger since PFHEs tend to be more compact and less expensive. Heaters (sodium to helium) are PCHE type HXs to enhance reliability. Heaters and the recuperator can be made of common high temperature steel such as 316L used for the recuperator in GT-MHR design. All of these compact HX designs use *mm* scale thick wall or fins to achieve high power density. Similar non-compact type of coolers as used in the 1996 GT-MHR design are also used for the MCGC PCS coolers. The volumes of coolers are calculated using the ratio of thermal power and the GT-MHR cooler volumes.

The turbomachinery sizing code uses simple design methods [22] to size turbines and compressors and calculate pressure losses. All the turbines and compressors are synchronous (3600 rpm) due to the large flow rate and size. Also the same dynamic pressure recovery ratios for turbine and compressor exits as GT-MHR are used. The sizes of stators and bearings are estimated according to power scaling from the corresponding GT-MHR and PBMR designs. Specific speed and diameters[23] for turbines and compressors are evaluated and fall into the optimized efficiency region.

The duct system sizing code calculates the size of connection ducts and pressure losses. All of the form losses and wall friction losses are accounted for in the pressure loss calculation. The total fractional pressure loss for all of the connection ducts is less than 4% of the system total pressure.

The material input code calculates figures of merit such as specific power density, specific steel input, and specific helium inventory. Specific power density is defined as the electrical power per unit of PCS volume. It is an indicator of material consumption and building volume. Specific steel input is defined as the steel mass per unit of electricity power. It is a direct indicator of major material cost for a PCS system. Specific helium inventory is defined as helium mass per unit of electricity power. It decides helium cost and storage volume requirements. Storage is required both for maintenance, and for power control, because power changes are achieved by changing the gas inventory. After sizing of each major component in the PCS, it is relatively straightforward to estimate specific power density and specific helium inventory. It is difficult to precisely account for the total material consumption without a detailed engineering design. However, it is possible to estimate the major material inputs for the PCS by including major PCS components such as the pressure boundary (pressure vessels and ducts), generator, turbomachinery, and heat exchangers.

### *II.C. PCU Arrangement*

Figure 4 shows the schematic flow diagram for the distributed three horizontal-shaft multiple-reheat cycle, using three sets of PCU modules (High Pressure (HP), Middle Pressure (MP), and Low Pressure (LP) ). Each set of PCU module contains a generator, a turbine, two compressors, and a heater and two cooler heat exchangers. All the components are located in separate vessels. The flow shown in red in the left part of this diagram forms the hot flow loop (not a closed loop, but connected to the cold loop in recuperator), within which high temperature helium flows in heaters, hot ducts, turbines, and the recuperator. The arrangement pattern shown in the diagram is optimized to minimize the total length of hot ducts, which are much more expensive than cold ducts and generate heat losses. All the hot ducts are concentric ducts and cooled by small flows of cold helium (10% of total flow) in the annulus outside hot inner ducts. The flow shown in blue going through coolers, cold ducts, compressors and cooling paths for hot ducts forms a larger cold loop. Note that the heaters (IHX) are located around the reactor vessel to minimize the primary system size and reduce sodium loop surface area.

In this design, the pressure boundary operates at, or slightly above, the compressor outlet temperature. This is a very low temperature, and thus the pressure boundary can be made from inexpensive steel. There is also a pressure difference between the cold helium next to the pressure boundary and the hot helium in the hot ducts inside, so the hot ducts and turbine casings must operate with some

pressure difference and stress too. However, insulation in these systems can allow the hot components to operate closer to the cold temperature than the hot temperature. The steady-state pressure difference between the hot and cold fluids is minimized.

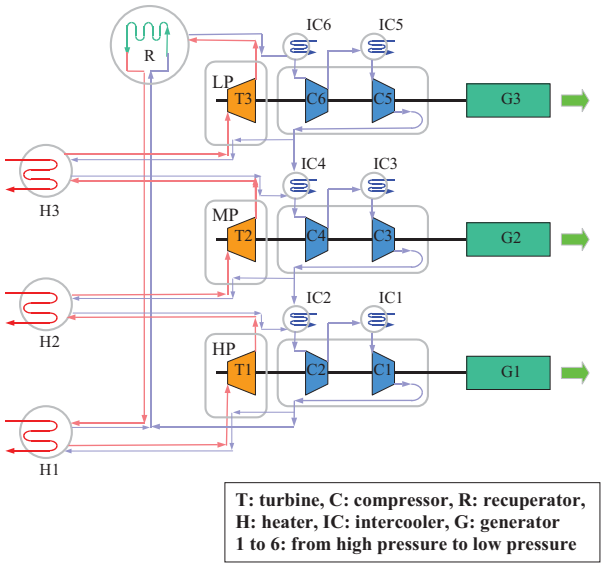


Fig. 4. Schematic flow diagram for the distributed three horizontal-shaft multiple-reheat cycle, using three PCU modules.

## III. REFERENCE DESIGN AND SENSITIVITY STUDY

The reference design is for an advanced loop type SFR as shown in Fig. 2, similar as the JSFR design but with the reactor inlet temperature increased from 395°C to 415°C. Thermal power affects the economics of scale. Larger plants tend to be less expensive in the sense of cost per kWh electricity generation. A 2400 MWt thermal power is chosen here to take advantage of economics of scale. The corresponding electricity power is around 1000 MWe.

Comparable parameters used in other helium Brayton cycles [18, 19, 20] and SCO2 cycles [9, 10] are assumed in the helium Brayton cycle calculations: i.e., the turbine adiabatic efficiency at 93%, the compressor adiabatic efficiency at 90%, and the recuperator effectiveness at 95%. Recent helium compressor R&D work for Japan's GTHTR300 demonstrates that 90% of adiabatic efficiency is achievable for large helium compressors.[24] The compressor inlet temperature is assumed to be 30°C. The total relative pressure loss is around 10%.

System pressure is a parameter that can be optimized according to cycle design, the state-of-the-art for high-temperature materials subjected to high pressure, and overall cost. Higher system pressure decreases the component equipment size, such as the heat exchangers, turbomachinery, and gas ducting system so that the power density can be increased. If similar component sizes are kept, higher pressure can reduce relative pressure loss so that the cycle thermal efficiency is increased. Higher system pressure complicates the heater design because the primary sodium loop usually has low pressure and the heaters operate under the highest temperature and largest pressure difference in the entire PCS. Higher system pressure also increases helium leakage. GT-MHR[18] uses a peak pressure of 7.24 MPa and PBMR[19] uses a peak pressure of 9 MPa. Superheated steam cycles widely used for SFR designs have steam pressures between 15 MPa to 20 MPa, i.e., 15 MPa for ALMR[25], 18.5 MPa for EFR[1], and 19.2 MPa for JSFR[3]. The MCGC system is an indirect cycle, with the entire pressure boundary operating at low temperature - the compressor outlet temperature; therefore, it can use higher pressure economically. This paper compares 10 MPa and 20 MPa options. Detailed economic analysis is needed to choose the optimal pressure.

Table I summarizes the power conversion design parameters for two system pressure options and the reference GT-MHR design, and Table II gives the power conversion design main system sizes, power density, specific metal mass and specific helium mass. The MCGC cycles use three distributed PCUs with horizontal shafts and each has one turbine and two compressors. For the turbine inlet temperature of 535ºC, the thermal efficiency is 42.4% which is very close to 42% of the JSFR steam cycle thermal efficiency. The PCS power densities are 220 kW(e)/m$^3$ for the 10 MPa case, and 280 kW(e)/m$^3$ for the 20 MPa case; and the corresponding specific metal masses are 9.6 MT/MWe and 11 MT/MWe, respectively.

The PCUs power density directly determines structure and building size, therefore the material and construction costs, and construction time. MCGC systems shown in Table II have similar or higher power densities depending on the system pressure than the GT-MHR PCU system, even though they operate with SFR-relevant temperatures. The higher power density for the 20 MPa MCGC system is achievable for several reasons: much larger power, higher system pressure, and a smaller relative recuperator power. The MCGC systems have similar or smaller PCU vessel diameters as GT-MHR and the MCGC PCU shafts are shorter than the GT-MHR PCU shaft. The MCGC turbines and compressors are larger in diameters than GT-MHR ones due to larger mass flow rate. However, each MCGC turbomachine need much less number of stages than GT-MHR ones.

Besides power density, metal mass per unit electricity output for PCS is another important indicator for equipment cost. For PCUs, most of the metal used is steel. As shown in Table II, MCGC PCUs for the SFRs use about 1/3 more metal per unit electricity output than GT-MHR. This is due to several reasons: (1) the SFR-MCGC systems have less thermal efficiency than the GT-MHR due to much lower heating temperature; (2) Distributed arrangement requires

much larger pressure boundary surface area than the integrated system like GT-MHR PCU uses; (3) Long connecting gas ducts (about 200 meter total hot duct and about 100 meter total cold duct) require large amount steel (about 30% of total PCS mass for the 10 MP case). However, the MCGC systems operate at much lower temperature than GT-MHR (535°C versus 850°C) so that the material and equipment cost could be lower. GT-MHR PCS is a direct cycle and requires nuclear grade equipment which tends to be substantially more expensive than non-nuclear equipments. Overally, it can be expected that the large MCGC PCS systems for the SFR designs could have similar or less specific cost than the GT-MHR PCS.

Comparing the two system pressure options shown in Table I, we keep the same thermodynamical parameters so that the high pressure case has more compact PCS design: smaller turbomachinery, smaller pressure vessels, and smaller gas duct. However, due to the increased pressure, the pressure boundary thickness needs to be increased, which results higher specific metal mass even with higher power density. Helium inventory also increases due to increased helium density. If we keep similar component power densities, we can increase the thermal efficiency. The optimal system pressure therefore needs to be selected according to detailed economic and safety analysis.

Table III shows parameter sensitivities on thermal efficiency for the 10 MPa system pressure case. Heat sink has large impact on the thermal efficiency. Turbomachinery efficiencies has important impact too. Increasing reactor outlet temperature, reducing heat sink temperature, improving component efficencies can further improve the thermal efficiency.

TABLE I

SFR MCGC System Design Parameters and Comparison with the GT-MHR PCU

| | SFR-MCGC Case 1 | SFR-MCGC Case 2 | GT-MHR |
|---|---|---|---|
| Thermal power (MW) | 2400 | 2400 | 600 |
| Primary max. /min. temperature (°C) | 550/415 | 550/415 | 848/488 |
| Turbine inlet/outlet temperature (°C) | 535/400 | 535/400 | 848/508 |
| Compressor inlet/outlet temperature (°C) | 30/67.7 | 30/67.7 | 26.4/110.3 |
| System pressure (MPa) | 10 | 20 | 7.24 |
| Number of PCU's | 3 | 3 | 1 |
| Numbers of turbines and compressors | 3/6 | 3/6 | 1/2 |
| Helium mass flow rate (kg/s) | 1096 | 1096 | 317 |
| Cycle pressure ratio (-) | 4.41 | 4.41 | 2.69 |
| Pressure loss fraction (-) | 0.102 | 0.1 | 0.07 |
| Thermal efficiency (-) | 0.424 | 0.424 | 0.48 |

TABLE II

SFR MCGC System Size Parameters and Comparison with GT-MHR PCUs

| | SFR-MCGC Case 1 | SFR-MCGC Case 2 | GT-MHR |
|---|---|---|---|
| PCU (HP, MP and LP) total length (m) | 33/34/35 | 32/32/33 | 38 |
| Turbine vessel (HP, MP and LP) diameter (m) | 4.6/5.0/5.4 | 4.2/4.5/4.9 | 7.2 |
| Generator vessel diameter (m) | 4.4 | 4.4 | 4.4 |
| Max. turbine (T3) tip diameter (m) | 2.98 | 2.44 | 1.783 |
| Number of stages for largest turbine (T3) | 3 | 4 | 11 |
| Max. Compressor (C6) tip diameter (m) | 2.55 | 2.12 | 1.684 |
| Number of stages for largest Compressor (C6) | 3 | 4 | 14 |
| The ratio of recuperator power over thermal power | 0.75 | 0.75 | 1.04 |
| PCUs power density (kW(e)/$m^3$) | 220 | 280 | 230 |
| Specific metal mass for PCUs (MT/MWe) (capacity factor: 0.9) | 9.6 | 11. | 7.5 |
| Specific helium inventory (kg/MWe) | 14. | 19. | 15.9 |

TABLE III

Thermal Efficiency Sensitivity with Major Parameters (Relative Change Relative to the 10 MPa Reference Design)

| Parameter change | Increasing Parameter | Decreasing Parameter |
|---|---|---|
| 10°C change of turbine inlet temperature (535°C*) | 1.2% | -1.4% |
| 10°C change of compressor inlet temperature (30°C) | -4% | 4% |
| 0.01 change of the total fractional pressure loss (0.1) | -0.9% | +0.9% |

| | | |
|---|---|---|
| 0.01 change of turbine efficiency (0.93) | 1.4% | -1.7% |
| 0.01 change of compressor efficiency (0.9) | 1.4% | -1.4% |
| 0.01 change of recuperator effectiveness (0.95) | 0.7% | -0.9% |

* values shown in brackets are reference design parameters

## IV. FURTHER DISCUSSIONS

### *IV.A. IHX Break Analysis*

Although PCHE type of IHXs are very robust and reliable, a very small break still could happen in a large SFR plant. Unlike a steam cycle where ingressed water/steam will react locally with sodium, the ingressed high pressure helium could go into the core and cause positive reactivity. SFRs usually are designed with strong net negative reactivity feedback, a small void fraction therefore can be easily compensated by other negative reactivity effects so that a small break could be well tolerated without shuting down the reactor. For a large break, a gas-liquid separator[12] located between the IHX and primary pump will remove most of helium from the primary system.

Detailed system analyses are necessary to obtain detailed consequences for different IHX break scenarios, which will be performed in the future study. A scaling based method could provide preliminary insights. By assuming critical flow from the break and homogenous two phase flow in the primary loop, averaged void fraction can be estimated for different break sizes. Since the PCHEs have flow channels at the order of mm, only mm scale break could happen with some creditable chance. Fig. 5 shows a single point break with high pressure helium flowing into a sodium channel. The total helium flow rate in the Brayton cycle is about 1000 kg/s. The leakage rate for mm scale break is about 0.01 kg/s and the resulting void fraction in the reactor core is at the order of 1%. Such small leakage rate won't affect the operation of the Brayton cycle. However, local concentration of helium bubble in subassemblies could increase clad temperature and bring positive reactivity. 1 cm scale break should be extremely impossible for a well designed compact heat exchanger. For worst case scenario, a large 1 cm scale break will result in 20% to 30% maximal void fraction in the core if no gas-liquid separator is used.

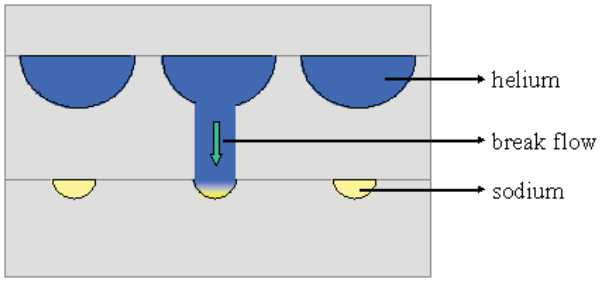


Fig. 5. Single point break with high pressure helium flowing into a sodium channel.

To analyze the reactivity effect due to void fraction, a specific core design is needed. Here we use an advanced SFR design shown in Fig. 6 as an example. This design uses radial and axial enrichment zoning and slight moderation near the reflectors to flatten the power profile.[26] Like most SFR designs, this design has a positive sodium density coefficient. The positive reactivity feedback is a direct consequence of neutron energy spectrum hardening resulting from the loss of the slight neutron down-scattering and capture provided by the sodium coolant. When the spectrum hardens, the lack of down scattering causes the number of neutrons above the fission threshold of fertile isotopes (U-238 and minor actinides) to increase. An increase in above-threshold fissions causes an increase in the neutron multiplication contribution of these fertile isotopes. The loss of sodium also influences the amount of neutron leakage from the core which increases as the down-scattering from sodium atoms decreases. The resulting effect of the spectrum hardening on core reactivity is dominated by the spatial dependence of this neutron leakage.

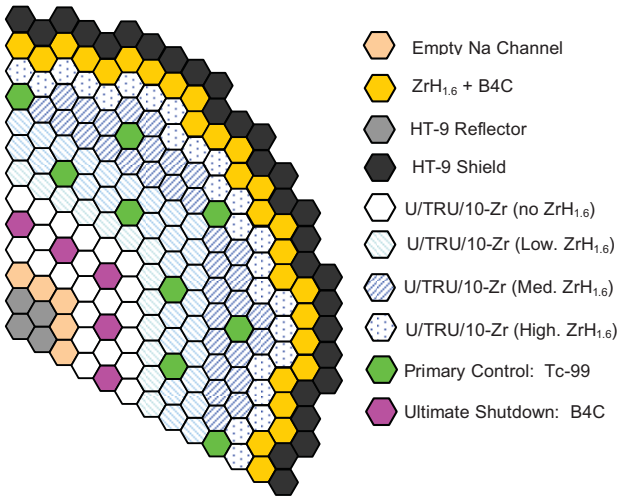


Fig. 6. An advanced SFR core design.

The MC2-2/DIF3D/REBUS-3 code package was used to estimate the sodium densitity reactivity in the refered design. The calculations show that a change in sodium density of 30% would cause about 1.5 percentage change in reactivity. Assuming a delayed neutron fraction typical of SFR's (~0.0035 [27]), this would correspond to about $ 4.0 of reactivity insertion. Therefore it is necessary to have gas-liquid separators or other design features to prevent such large void formed in the core. However, as can be seen from Fig. 7, for a small decrease in sodium density, as a result of a small leak, the reactivity insertion is about 0.04% or approximately $ 0.1, which can be manageable through

passive reactivity feedback or active control rod moving.

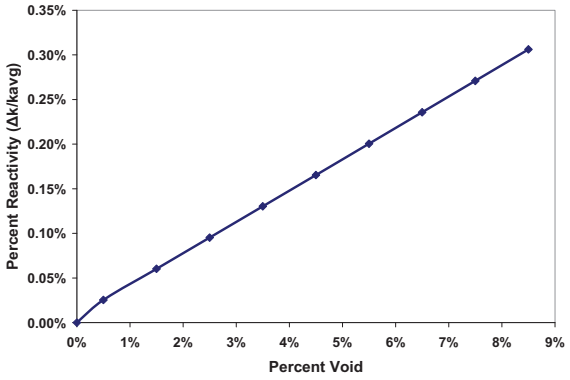


Fig. 7. Sodium density worth curve (0-10% density change).

### *IV.B. Additional Research Needs*

As we discussed previously, multiple reheat helium Brayton cycle development is mainly based on non-reheat helium Brayton cycle development for HTGRs. Most of the major technology issues are the same, such as helium turbomachinery development, advanced bearing and sealing, high temperature compact heat exchangers, etc. The multi-reheat helium Brayton cycle systems for SFRs have much lower maximum temperatures than the Brayton cycles for HTGRs. Therefore less expensive conventional high temperature alloys can be used for heat exchangers and no turbine blade cooling is needed. Besides these common techniques, there are unique issues for sodium heating MCGC systems, for example, sodium-to-helium heat exchangers and more complex systems. More detailed design work for the SFR MCGC systems needs to be performed as part of advanced SFR plant design (Fig. 2). Dynamical models need to be developed so that transient behaviors during startup, shutdown, and load changes can be studied. Projects to design, test, and analyze the sodium-to-helium compact heat exchangers will solve the feasibility issue of using sodium-to-helium compact heat exchangers.

## V. CONCLUSIONS

A multiple reheat helium Brayton cycle can be adopted for an advanced loop type SFR to eliminate the intermediate sodium heat transfer loop so that the plant economics, reliability and safety could be substantially improved. The improvements mainly come from three aspects: (1) elimination of the intermediate sodium heat transfer loop has large cost saving and greatly reduce the sodium leakage probability; (2) removing water-sodium reaction from accident consideration significantly improves the plant safety and reduces the cost of related safety mitigation systems; (3) closed gas Brayton cycles cost less to build than steam cycles. The reference designs achieve a 42.4% thermal efficiency for 550°C reactor outlet temperature, very close to the JSFR design. Although substantial R&D works are necessary to further develop this technology, multiple reheat helium Brayton cycles could help SFRs overcome some of the largest economical and safety concerns. Synergy with HTGR Brayton cycles work could greatly accelerate the development of the multiple reheat Brayton cycles for SFRs.

## ACKNOWLEDGMENTS

This work was supported through INL Laboratory Directed Research and Development program under DOE Idaho Operations Office Contract DE-AC07-05ID14517. The design work was mainly based on the study the primary author performed at UC Berkeley with Prof. Per F. Peterson.

## REFERENCES

1. J.C. LEFEVRE, C.H. Mitchell, G. Hubert, "European Fast Reactor Design," *Nuclear Engineering and Design*, **Vol. 162**, pp 133-143 (1996).

2. IAEA, Status of Liquid Metal Cooled Fast Reactor Technology, IAEA-TECDCC-1083, ISSN 1011-4289, (1999).

3. Y. SHIMAKAWA, et. al., "An Innovative Concept of a Sodium-Cooled Reactor to Pursue High Economic Competitiveness," *Nuclear Technology*, **Vol. 140**, No. 1, pp. 1-17 (2002).

4. M. KONOMURA and M. Ichimiya, "Design Challenges for Sodium Cooled Fast Reactors," *Journal of Nuclear Materials*, **Vol. 371**, pp. 250-269 (2007).

5. J. GUIDEZ, L. Martin, S.C. Chetal, P. Chellapandi, B. Raj, "Lessons Learned From Sodium-Cooled Fast Reactor Operation and Their Ramifications for Future Reactors with Respect to Enhanced Safety and Reliability," *Nuclear Technology*, **Vol. 164**, No 2, pp. 207-220 (2008).

6. M. MATSUURA, M. Hatori, M. Ikeda, "Design and Modification of Steam Generator Safety System of FBR MONJU," *Nuclear Engineering and Design*, **Vol. 237**, n 12-13, pp. 1419-1428 (2007).

7. N.E. TODREAS, "Thermal Hydraulic Challenges in Fast Reactor Design," *Proceedings of the 12th International Topic Meeting on Nuclear Thermal Hydraulics (NURETH-12)*, American Nuclear Society, Pittsburgh, Pennsylvania, USA (2007).

8. L.J. KOCH, *Experimental Breeder Reactor-II (EBR-II), An Integrated Experimental Fast Reactor Nuclear Power Station,* American Nuclear Society (2006).

9. V. DOSTAL, P. Hejzlar, and M.J. Driscoll, "High Performance Supercritical Carbon Dioxide Cycle for Next-Generation Nuclear Reactors," *Nuclear Technology*, **Vol. 154**, pp. 265-282 (2006).

10. Y.I. CHANG, et. al., *Advanced Burner Test Reactor Preconceptual Design Report*, Argonne National Laboratory, ANL-ABR-1 (ANL-AFCI-173), Sept. 5 (2006).

11. J.H. CHOI, S.D. Suk, D. Cho, J.M. Kim, D. Hahn, J.H. Cahalan, "Capsule Test for Investigating Sodium-Carbon Dioxide Interaction," *Proceedings of 2006 International Congress on Advances in Nuclear Power Plants (ICAPP '06)*, American Nuclear Society, Reno, NV, USA (2006).

12. M. SAEZ, D. Haubensack, N. Alpy, A. Gerber, F. David, "The Use of Gas Based Energy Conversion Cycles for Sodium Fast Reactors," *Proceedings of 2008 International Congress on Advances in Nuclear Power Plants (ICAPP'08),* American Nuclear Society, Anaheim, CA, USA (2008).

13. P.F. PETERSON, "Multiple-Reheat Brayton Cycles for Nuclear Power Conversion with Molten Coolants," *Nuclear Technology*, **Vol. 144**, pp. 279–288 (2003).

14. H. ZHAO, and P.F. Peterson, "Optimization of Advanced High-Temperature Brayton Cycles with Multiple Reheat Stages," *Nuclear Technology*, **Vol. 158**, pp. 145-157 (2007).

15. H. ZHAO, and P.F. Peterson, "Low-Temperature Multiple-Reheat Closed Gas Power Cycles for the AHTR and LSFR," *Proceedings of, 2006 International Congress on Advances in Nuclear Power Plants (ICAPP '06),* American Nuclear Society, Reno, NV, USA (2006).

16. H. ZHAO, and P.F. Peterson, "Multiple Reheat Helium Brayton Cycles for Sodium Cooled Fast Reactors," *Nuclear Engineering and Design*, **Vol. 238**, pp. 1535–1546 (2008).

17. H. ZHAO, H. Zhang, V.A. Mousseau, and P.F. Peterson, "Improving SFR Economics through Innovations from Thermal Design and Analysis Aspects," *Proceedings of 2008 International Congress on Advances in Nuclear Power Plants (ICAPP'08)*, American Nuclear Society, Anaheim, CA, USA (2008).

18. M.P. LABAR, "The Gas Turbine–Modular Helium Reactor: A Promising Option for Near Term Deployment," *Proceedings of 2002 International Congress on Advanced Nuclear Power Plants (ICAPP '02)*, American Nuclear Society, Hollywood, Florida, USA (2002).

19. R.A. MATZIE, "Pebble Bed Modular Reactor (PBMR) Project Update," *Proc., 2004 International Congress on Advances in Nuclear Power Plants (ICAPP '04),* American Nuclear Society, Pittsburg, Pennsylvania, USA (2004).

20. K. KUNITOMI, S. Katanishi, S. Takada, T. Takizuka, X. Yan, "Japan's Future HTR - the GTHTR300," *Nuclear Engineering and Design*, **Vol. 233**, pp. 309-327 (2004).

21. W.M. KAYS and A.L. London, *Compact Heat Exchangers,* 3rd ed., McGraw Hill Book Company, New York (1984).

22. L. FIELDING, *Turbine Design: The Effect of Axial Flow Turbine Performance of Parameter Variation*, ASME Press, New York (2000).

23. O.E. BALJE, *Turbomachines: A Guide to Design, Selection and Theory*, John Wiley and Sons, New York (1981).

24. X. YAN, T. Takizuka, K. Kunitomi, H. Itaka, K. Takahashi, "Aerodynamic Design, Model Test, and CFD Analysis for A Multistage Axial Helium Compressor," *Journal of Turbomachinery*, **Vol. 130**, 3, pp. 1-12 (2008).

25. E.L. GLUEKLER, "U.S. Advanced Liquid Metal Reactor (ALMR)," *Progress in Nuclear Energy*, **Vol. 31**, No. 1, pp. 43-61 (1997).

26. S.E. BAYS, H. Zhang, H. Zhao, "the Industrial Sodium Cooled Fast Reactor," *Advances in Nuclear Fuel Management IV (ANFM-IV)*, American Nuclear Society, Hilton Head Island, SC, April 12-15, 2009.

27. D.C. WADE, R.N. Hill, "the Design Rationale of the IFR," *Progress in Nuclear Energy*, **Vol. 31**, No. ½, pp. 13-42 (1997).